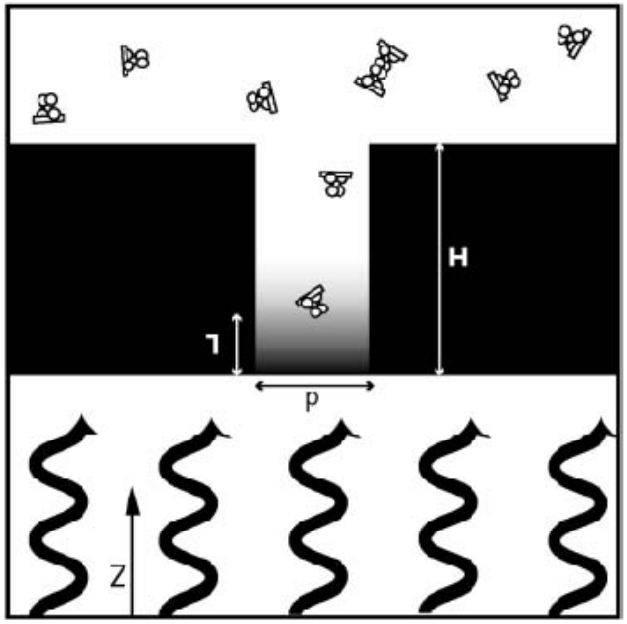

Zero-Mode Waveguides for Single-Molecule Analysis at High Concentrations

Cha Seoncheol
Sogang University, Department of Physics, Soft Matter Optical Spectroscopy

Review
Fluorescence Correlation Spectroscopy

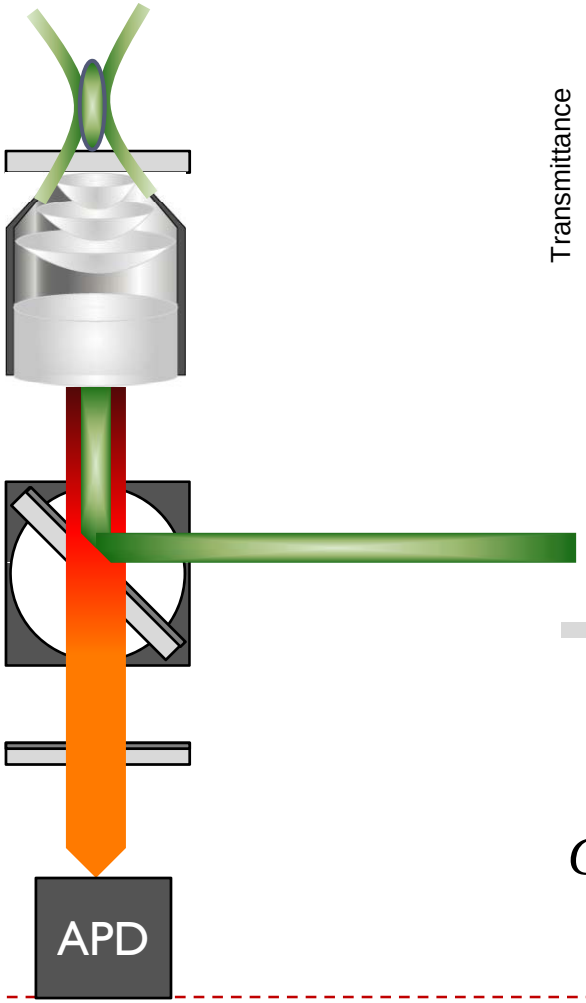

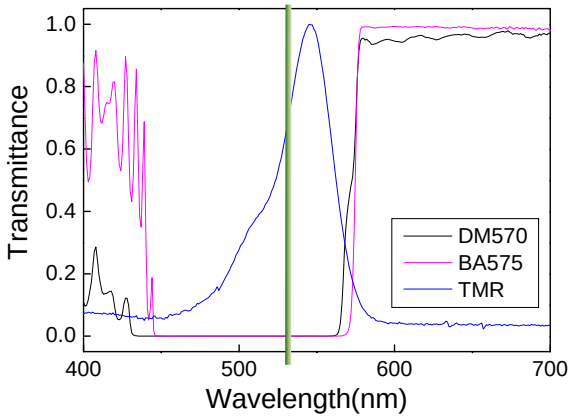

Laser Source

Autocorrelation function

$$G(\tau) = \frac{< \delta F(t) \delta F(t+\tau) >}{< F(t) >^2}$$

Review
Fluorescence Correlation Spectroscopy

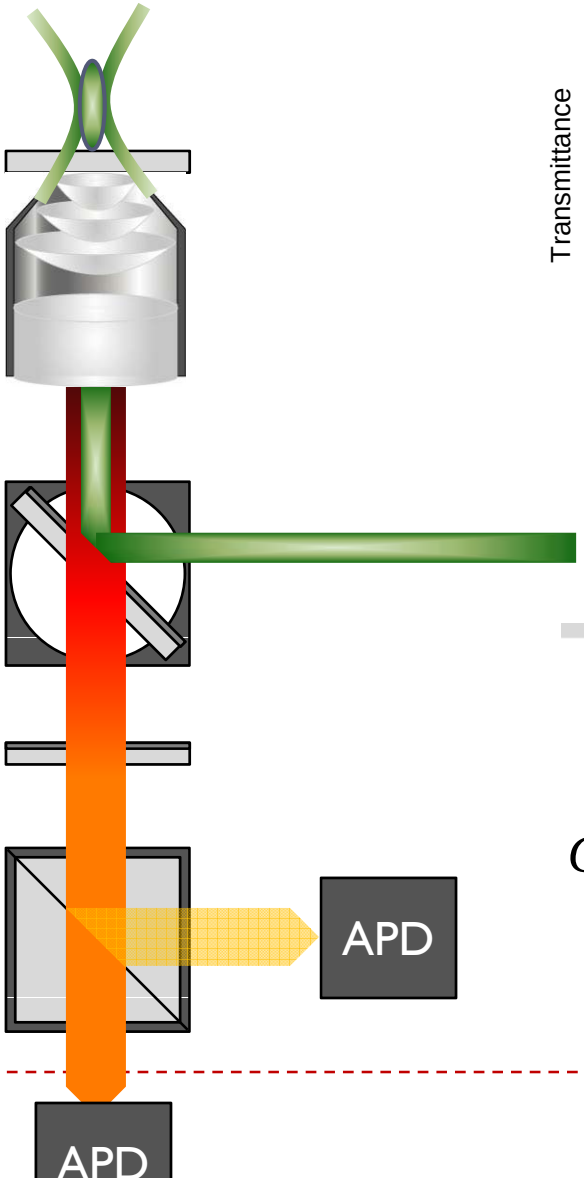

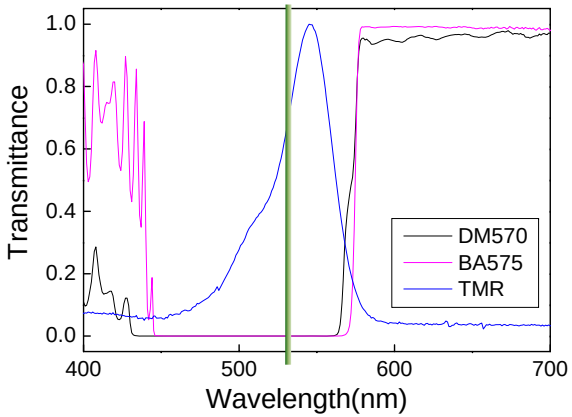

Laser Source

Cross Correlation function

$$G(\tau) = \frac{< \delta F_1(t) \delta F_2(t+\tau) >}{< F_1(t) >< F_2(t) >}$$

Review
Fluorescence Correlation Spectroscopy

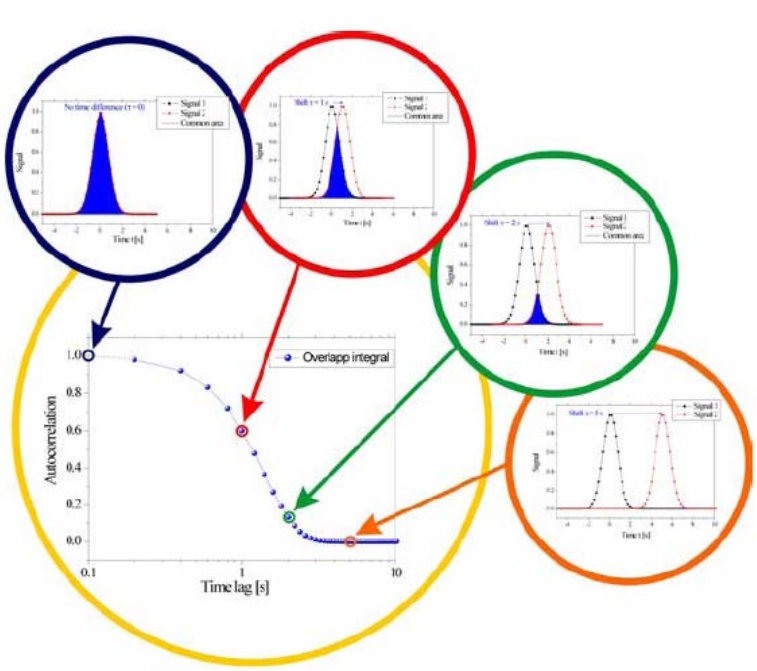

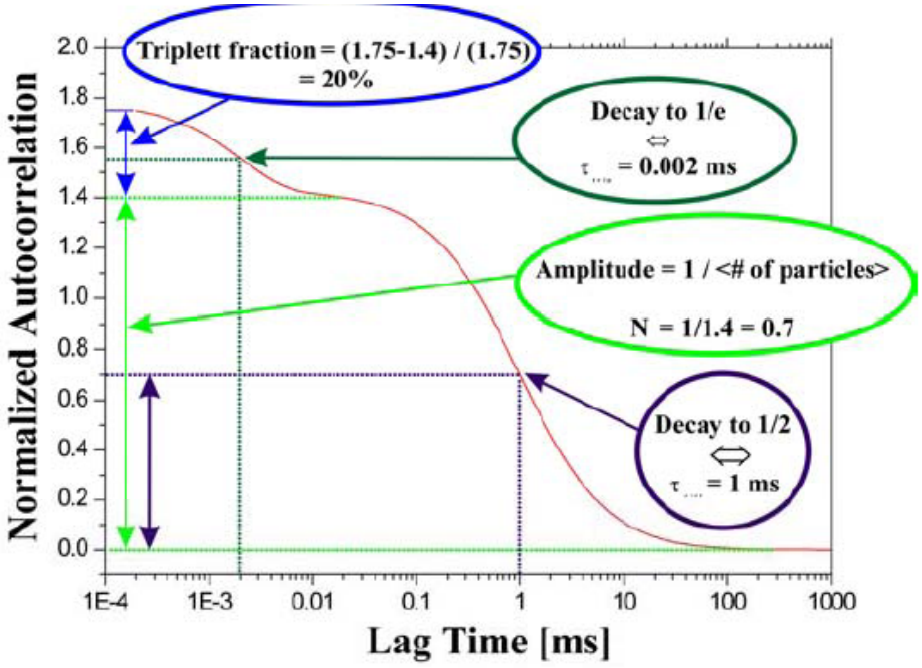

P.Schwille., *Biophysics Textbook Online* ***(2001).***

Review
Single Molecule Spectroscopy

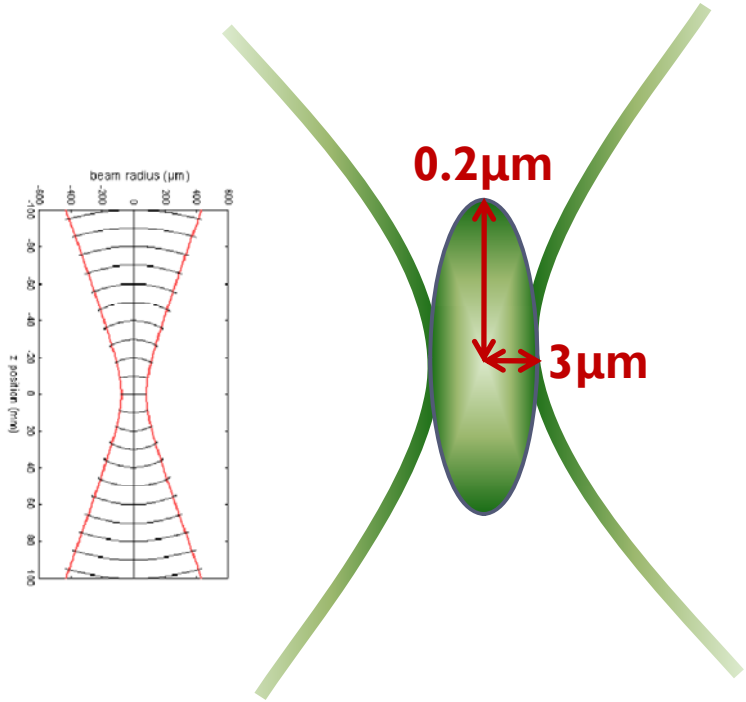

Considering 1n mol/L solution

$V_{eff} = \pi^{3/2} r_0^2 z_0 \sim 10fL$

1n mol/L $\cdot V_{eff} \cdot N_a \sim 6$

roughly six per volume element

In 100pm ~ 1nm range,
This method is able
to show single molecule dynamics

Why
Limitation of FCS

Zero-Mode Waveguides for Single-Molecule Analysis at High Concentrations

M. J. Levene,[1] J. Korlach,[1,2] S. W. Turner,[1*] M. Foquet,[1]
H. G. Craighead,[1] W. W. Webb[1†]

Optical approaches for observing the dynamics of single molecules have required pico- to nanomolar concentrations of fluorophore in order to isolate individual molecules. However, many biologically relevant processes occur at micromolar ligand concentrations, necessitating a reduction in the conventional observation volume by three orders of magnitude. We show that arrays of zero-mode waveguides consisting of subwavelength holes in a metal film provide a simple and highly parallel means for studying single-molecule dynamics at micromolar concentrations with microsecond temporal resolution. We present observations of DNA polymerase activity as an example of the effectiveness of zero-mode waveguides for performing single-molecule experiments at high concentrations.

Why
Previous approaches to overcome limitation of FCS

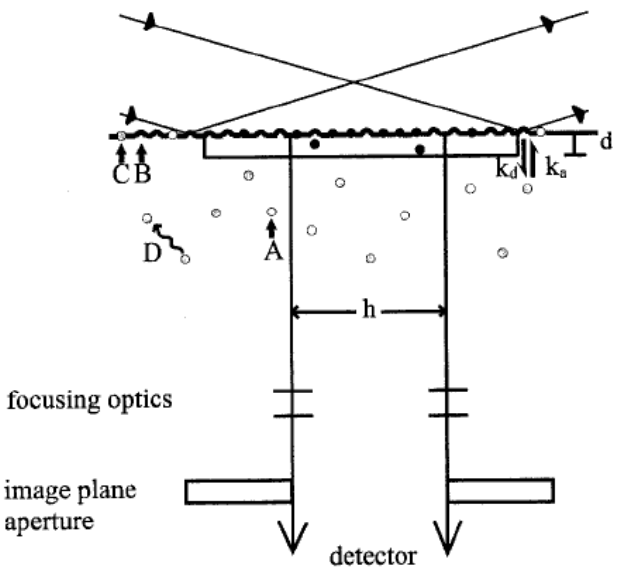

FIGURE 1 Schematic of TIR-FCS. Fluorescent molecules in solution, A, reversibly bind to free surface sites, B, forming complexes C. The association and dissociation kinetic rate constants are k_a and k_d, respectively. The diffusion coefficient of ligands in solution is D. Molecules bound or close to the surface are illuminated by an evanescent intensity of depth d. Fluorescence is measured from a surface area of h^2 through an aperture placed at an intermediate image plane. In this work, it is assumed that $h \gg d$ and that the surface binding sites and surface-bound complexes are not laterally mobile along the surface. Molecules fluoresce only when they are bound or close to the surface. Fluctuations in the measured fluorescence are autocorrelated. The fluorescence fluctuation autocorrelation function, $G(\tau)$, depends on k_a, k_d, A, D, d, and $S = B + C$.

T. E. Starr, N. L. Thompson, *Biophys. J.* ***80, 1575 (2001).***

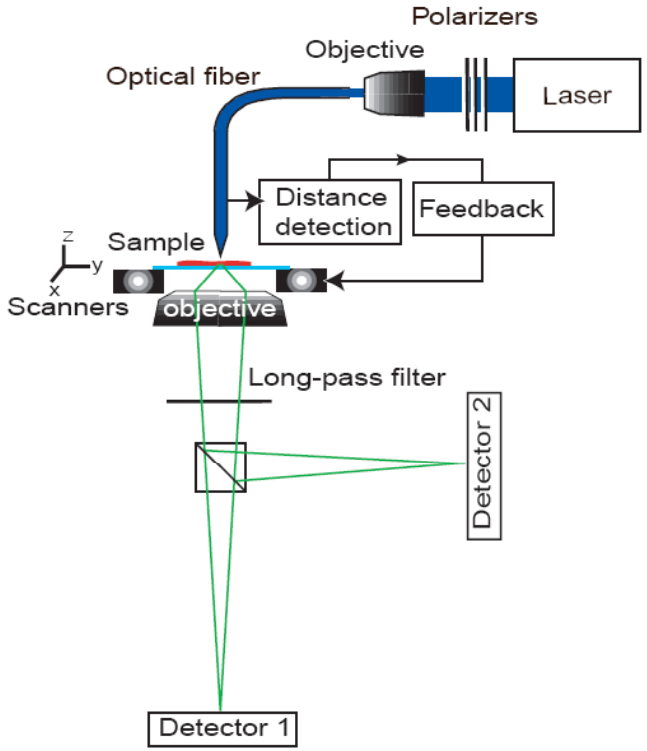

Fig. 2. Schematic lay out of a near-field scanning optical microscope. The NSOM probe is a tapered optical fiber (Fig. 3A). Laser light is coupled into the fiber and is used to excite fluorophores as the probe scans the sample surface. The probe-sample distance is maintained constant at <10 nm during scanning by shear-force-based distance detection in combination with an electronic feedback system controlling the piezoelectric scan stage. Fluorescence is collected by a conventional inverted microscope. Dual-channel optical detection allows wavelength and/or polarization discrimination.

F. de Lange *et al., J. Cell Sci.* ***114, 4153 (2001).***

Review
Single Molecule Spectroscopy

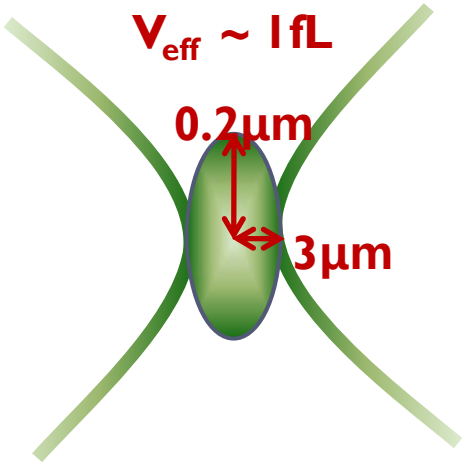

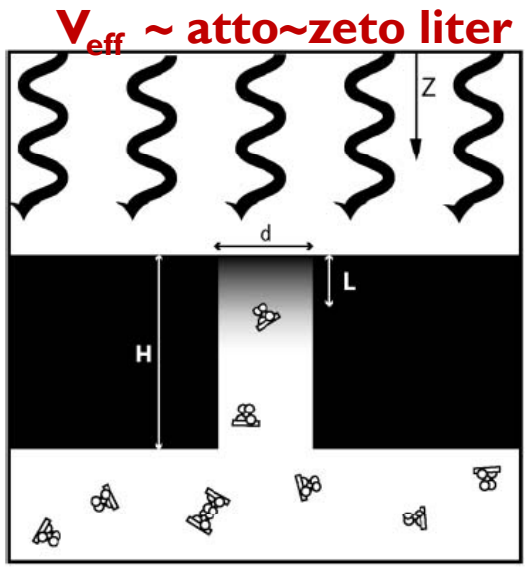

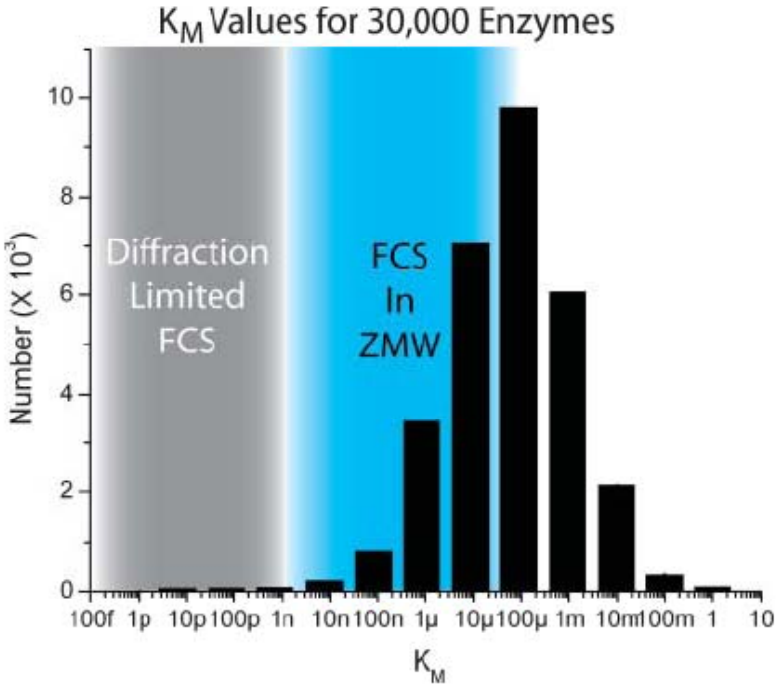

FIGURE 2 Histogram of K_M values for 30,000 enzymes taken from the Brenda Database (www.brenda.uni-koeln.de). The effective concentration ranges for diffraction limited and zero-mode waveguide FCS are shown in blue and red, respectively. Kinetics for the vast majority of enzymes are out of reach for diffraction limited FCS. FCS is not yet a viable tool above the 100 μM regime.

K.T.Samiee, et al., *Biophys. J.* ***88, 2145 (2005).***

How
Setup

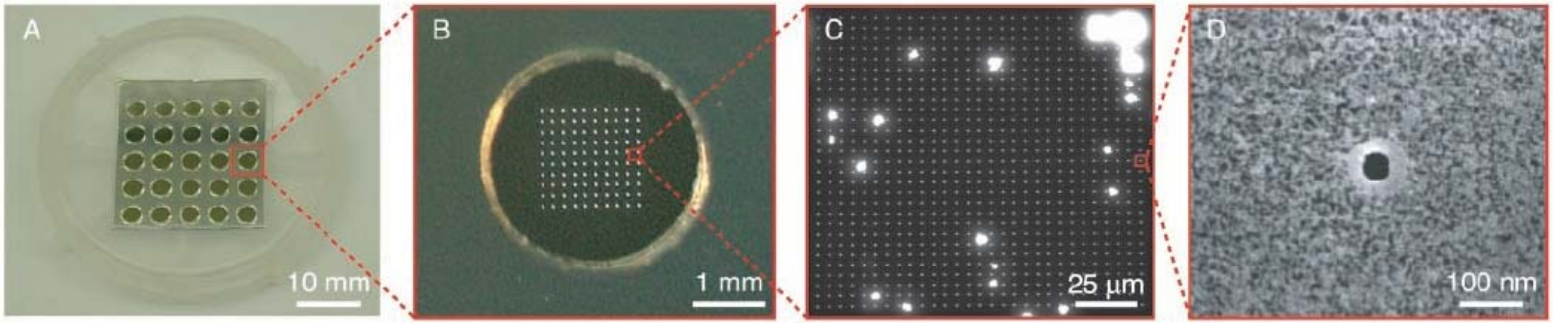

Fig. 3. A fused silica coverslip with zero-mode waveguides arrays. (**A**) The coverslip, with overlying gasket to isolate arrays for individual experiments. Successive increases in scale are shown in (**B**) to (**D**). A scanning electron microscope image of an individual waveguide is shown in (D). The bright spots in (C) correspond to defects in the metal film. The large bright pattern in the upper right corner is a coded orientation marker.

Fig. 1. An apparatus for single-molecule enzymology using zero-mode waveguides.

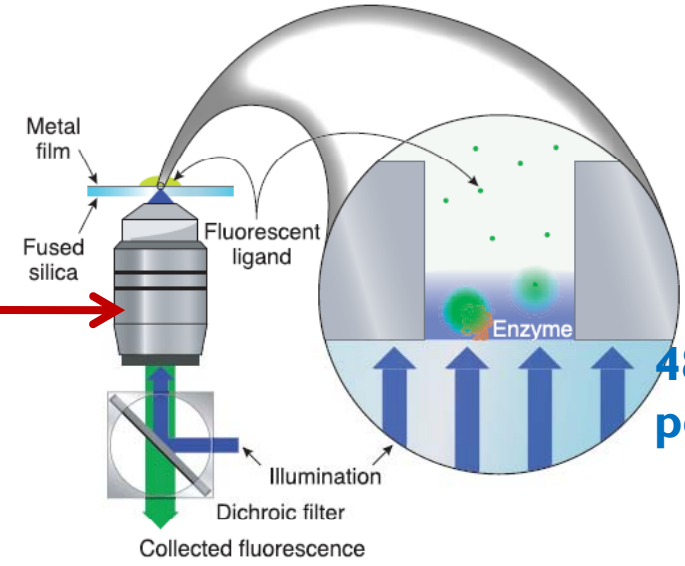

60x water immersion (NA = 1.2)

488nm circularly polarized light

How
Zero-Mode Waveguide (Example)

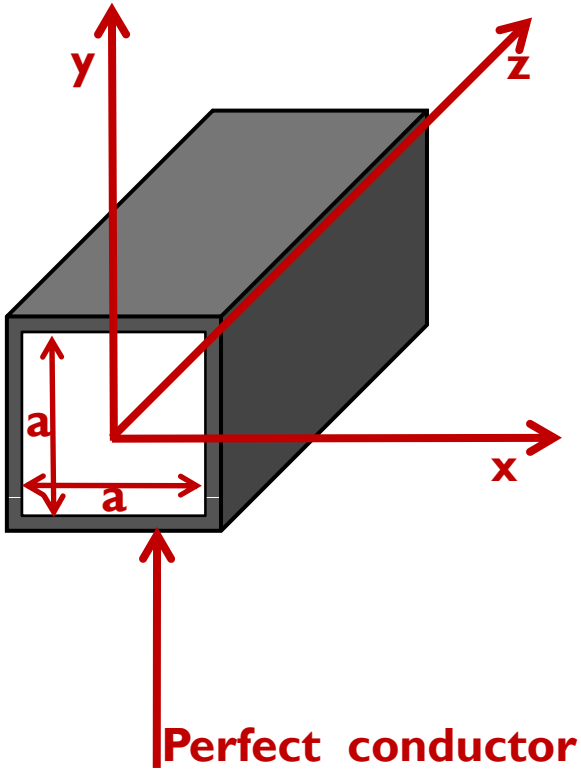

$$(\nabla^2 + \mu\varepsilon\omega^2)\begin{Bmatrix}\vec{E}\\ \vec{B}\end{Bmatrix} = 0$$

$$\vec{E}(x,y,z,t) = \vec{E}(x,y)e^{\pm i(kz-\omega t)}$$
$$\vec{B}(x,y,z,t) = \vec{B}(x,y)e^{\pm i(kz-\omega t)}$$

$$[\nabla_t^2 + (\mu\varepsilon\omega^2 - k^2)]\begin{Bmatrix}\vec{E}\\ \vec{B}\end{Bmatrix} = 0$$

$$\mu\varepsilon\omega^2 - k^2 \equiv \gamma^2 > 0 \quad \textbf{By B.Cs}$$

So, this equation has the modes .

Jackson (1999)

How
Zero-Mode Waveguide (Example)

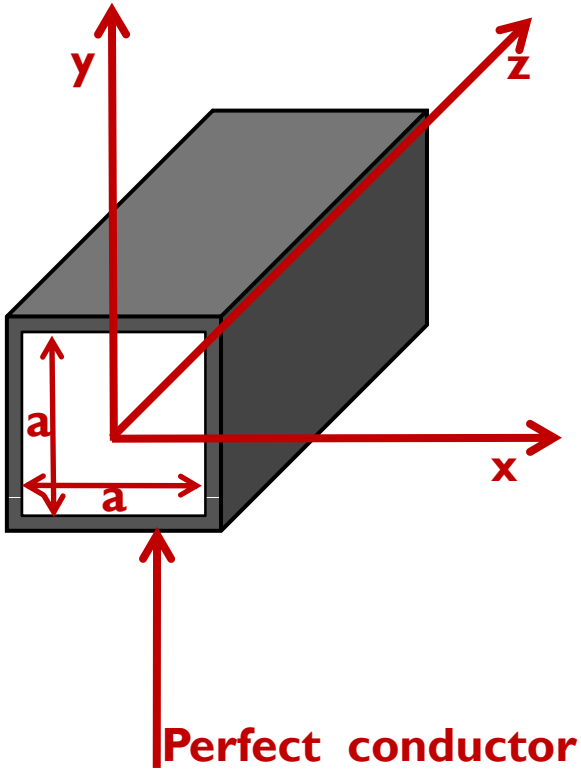

$$[\nabla_t^2 + \gamma_m]\psi_m = 0 \qquad k_m^2 = \mu\varepsilon\omega_m^2 - \gamma_m^2$$

Define $\omega_m = \dfrac{\gamma_m}{\sqrt{\mu\varepsilon}}$

From B.Cs $\gamma_m^2 = \dfrac{\sqrt{2}\pi^2 m^2}{a^2}$

$$\lambda_m \sim a$$

$$k = 2\pi\sqrt{\frac{1}{\lambda^2} - \frac{1}{\lambda_m^2}}$$

For longer wavelength (λ_m>a) are evanescent and their intensity decays exponentially along the length z of the guide

$$I(z) \propto e^{ikz}$$

Jackson (1999)

How
Zero-Mode Waveguide (Example)

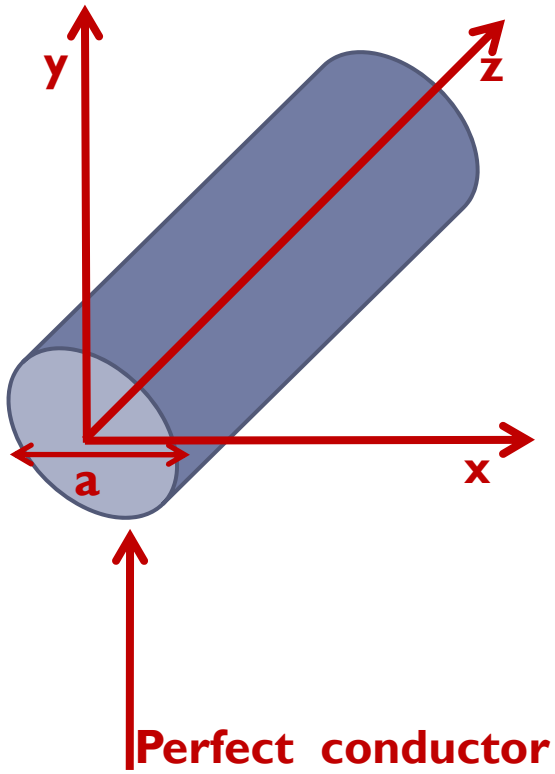

For circular waveguide case,

$$k = 2\sqrt{\frac{1}{\lambda^2} - \frac{1}{1.7d}}$$

$$I(z) \propto e^{ikz}$$

How
Zero-Mode Waveguide

For

Real Metal (Skin depth Effect)

-> Solving by Numerical Method

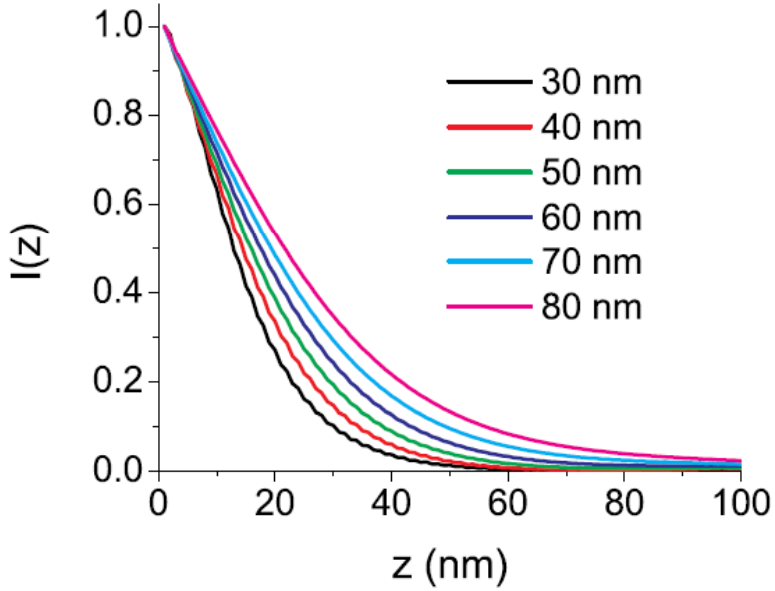

Calculation
Coupling Efficiency

radiative rate of a dipole

$\propto$ density of photonic states available for emission

Approximation : $k_r(z) \sim p(z)$

$$Q(z) = \frac{k_r(z)}{k_r(z) + k_{nr}} \approx \frac{p(z)}{p(z) + C}$$

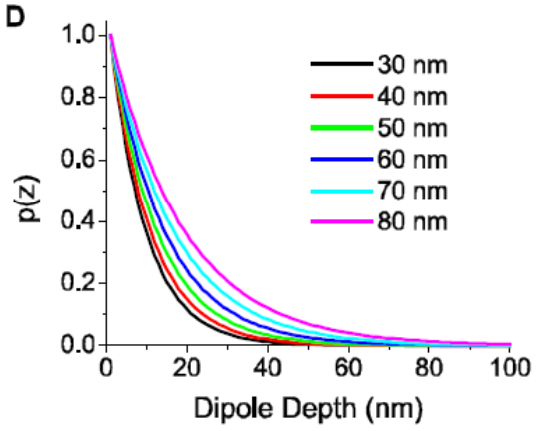

constant such that
Q(0) equals the quantum yield

p(z) : Averaging over all dipole orientations yields

Calculation
Effective Volume

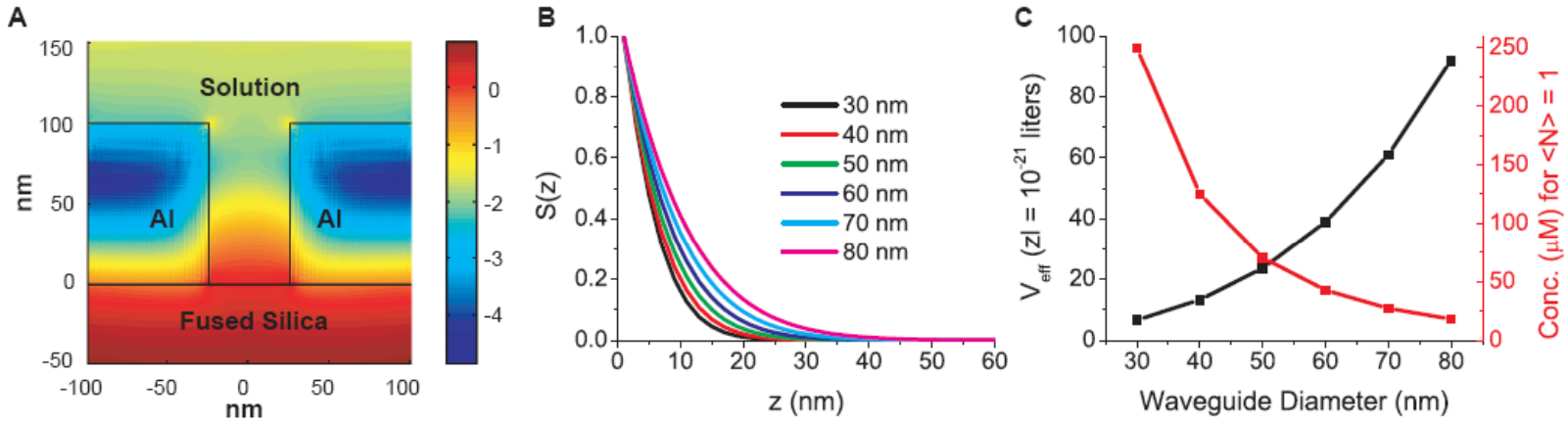

Fig. 2. (A) Three-dimensional finite-element time-domain simulation of the intensity distribution (log scale) for a zero-mode waveguide 50 nm in diameter and 100 nm long. (B) $S(z)$ curves for different waveguide diameter, d. (C) V_{eff} and the corresponding concentration for which there is, on average, one molecule in the volume ($\langle N \rangle = 1$).

$$S(z) = I(z)\,p(z)\,\frac{p(z)}{p(z)+C}$$

$$V_{eff} = \frac{\pi d^4}{4}\,\frac{\left(\int S(z)dz\right)^2}{\int S^2(z)dz} = \frac{1.56\pi L^3\lambda^2}{\lambda^2 - 36L^2} \qquad V_{eff}\,|_{L=14m} \sim \frac{1.56\pi L^3\lambda^2}{\lambda^2 - 36L^2}\,|_{L=14m} \sim 14zl$$

Calculation
Correlation Function

1-Dimensional Diffusion

$$G(\tau) \propto \int_{\upsilon_L}^{\infty} \left(\int S(z)\cos(\upsilon z)dz\right)^2 e^{-\upsilon^2 D\tau} d\upsilon$$

by perfect conductor approximation

$$G(\tau) = G_0\left[\frac{\pi}{4}\left((1-2\frac{\tau_d}{\tau})e^{\frac{\tau_d}{\tau}} erfc\left(\sqrt{\frac{\tau_d}{\tau}} - \frac{2}{\sqrt{\pi}}\left(\frac{\tau_d}{\tau}\right)^{-1/2}\right)\right) - \sqrt{\frac{\tau_d}{\tau}}\frac{erf(R)}{(1+R^2)^2}\right]$$

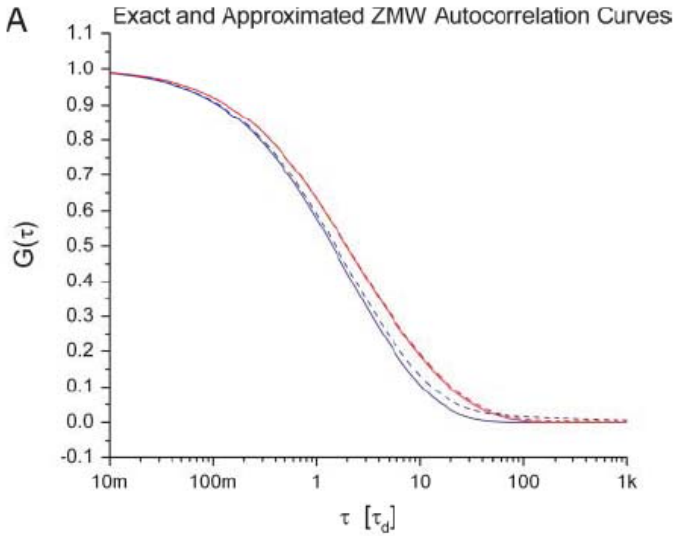

K.T.Samiee, et al., *Biophys. J.* ***88, 2145 (2005).***

Results
Correlation Function

R110dCTP : Rhodamine green + dCTP

$$G(0) = \frac{N}{(N+B)^2}$$

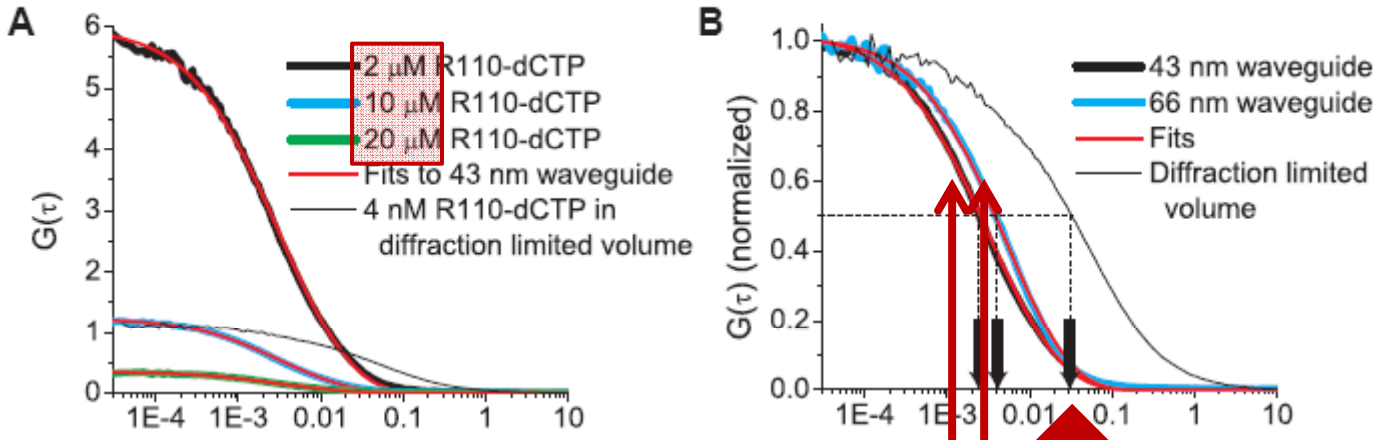

Free parameter is only waveguide diameter in fits

Zero-Mode Waveguide increases temporal resolution significantly

Results
Correlation Function

Results
Correlation Function

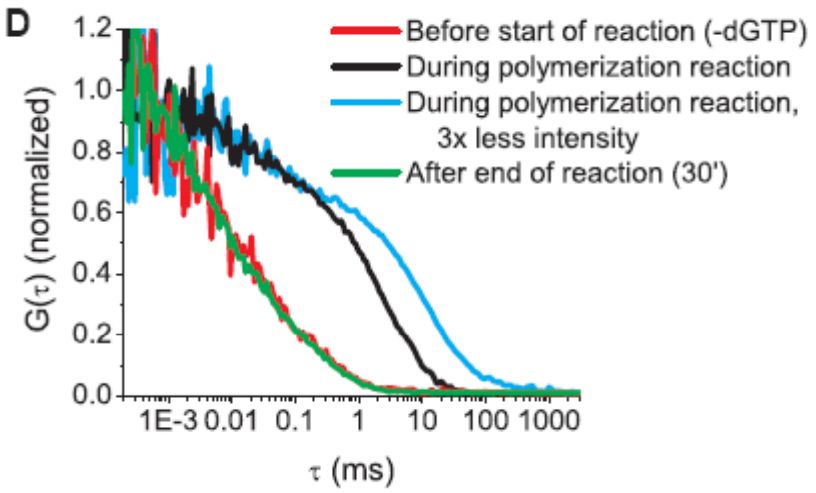

Fig. 4. (**A**) FCS curves for various concentrations of R110-dCTP in the same waveguide with fits to a 43-nm-diameter guide. (**B**) Normalized FCS curves of 10 μM R110-dCTP in two different sizes of waveguides. Arrows indicate the average residence times for molecules in the observation volumes. Curves from 4-nM dye in a diffraction-limited focal spot are shown in (A) and (B) for comparison. (**C**) Time trace and (**D**) FCS curves from single-molecule DNA polymerase activity inside a zero-mode waveguide. Incorporation events and subsequent photobleaching of coumarin-dCTP appear as distinct fluorescence bursts in the black time trace (10-ms time bins). This results in a long-time shoulder in the corresponding FCS curves during polymerization (black and blue curves) in (D). Decreasing the intensity results in slower photobleaching as seen by the longer residence time in the blue curve. The red curves in (C) and (D) are the corresponding negative controls (absence of one native nucleotide) in the same waveguide before initiation of the reaction. The green curve in (D) is the control after the reaction has stopped.